Proceedings of the 9th International Conference on Cyclotrons and their Applications
September 1981, Caen, France

RECENT DEVELOPMENTS AT THE KVI CYCLOTRON

O.C. Dermois, A.G. Drentje, H.W. Schreuder.

Kernfysisch Versneller Instituut, Zernikelaan 25, 9747 AA Groningen, the Netherlands.

Abstract. - A fast, pneumatic driven tuning capacitor is described. A nonconventional type of control has been developed for the pneumatic action. A displacement of 40 mm is realised in 0.2 s. after the appearance of the control signal.

Beam phase pick-up electrodes for RF phase measurements have been incorporated in a new probe head for the cyclotron's main phase probe. The associated phase detector uses synchronous detection. Phase measurements can be made on

Studies are described regarding unexpectedly large energy spreads in the analysed beam. Tests were done using the magnetic spectrograph at 0^{o} as an energy detector in order to deduce the shape of the emittance at the exit slit of the analysing magnet. A significant second order aberration was observed; it could be reduced considerably by removing the shims from the magnets entrance boundary.

Fast pneumatically driven tuning capacitor. - The present motor driven capacitor of the cyclotron is rather slow. A new control system has been designed, which is more compatible with the frequency measurement system. The frequency of the cyclotron is sampled every 0.3 s. from which 0.1 s. is actually used for counting. The frequency error signal is used to control a capacitor plate and the shorting bars in the coaxial line. The position of the shorting bars influences the tuning range of the capacitor : 0.5 $^{o}/_{oo}$ at 4 MHz and 1.1 $^{o}/_{oo}$ at 13 MHz.

To take maximum advantage of the speed of the frequency measurement a control system has been developed which generates a new position signal for the capacitor after the detection of an error signal. This new position should ideally cancel the frequency error. The system [1] is shown schematically in fig. 1. The circuitry generating the frequency error signal has built-in features to meet the stability criteria for sampled systems.

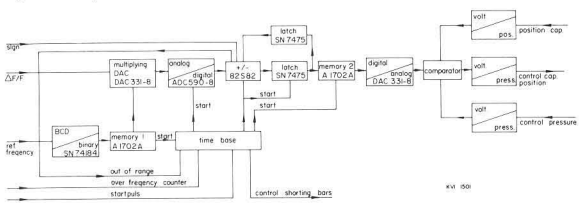

Fig. 1 : The electronics for the frequency control system. The frequency counter and additional circuitry generate a $\Delta F/F$ signal every 0.3 s. Memory 1 contains the information for the tuning range of the capacitor as function of the position of the shorting bar. Memory 2 contains the inverse of $\Delta C/C$ as a function of the position of the capacitor. Between the A.D.C. and memory 2 the add-substract logic generates the address of memory 2.

The most difficult part to realize is the power actuator for the capacitor. It has to move the capacitor plate over 4 cm within 0.2 s. The position accuracy and repeatability should be 0.1 mm. To meet these requirements the control of a pneumatic position servo cylinder has been modified. The new control part is shown in fig. 2. A balanced air distribution valve, 6, is powered by a magnet-coil system, 29 and 14, the speed of the valve stem is measured in a second magnet-coil system, 5 and 28, and used in a feedback loop. The air pressure at both sides of the main piston is measured too and converted. The difference of both pressure signals is used in a second feedback loop. The main feedback loop consists of a linear voltage-displacement transducer, connected to the cylinder stem, the signal of which is compared with the position signal generated by the system of fig. 1. Thus the

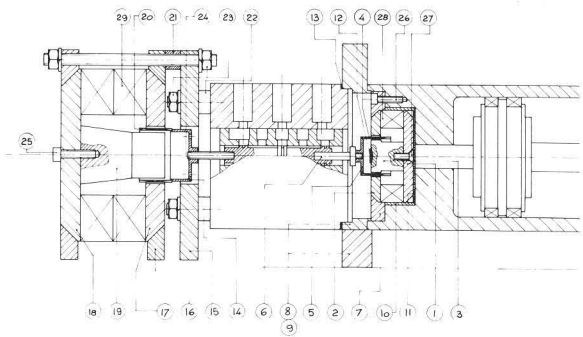

Fig. 2 : The rebuilt pneumatic position servo cylinder. The positioning mechanism has been removed and replaced by the speed control, 5 and 28, of the balanced valve, 6. This valve is driven by the power magnet, 29 and 14, and controls the air flow to the main cylinder. Two pressure-voltage transducers measure the pressure at both sides of the piston.

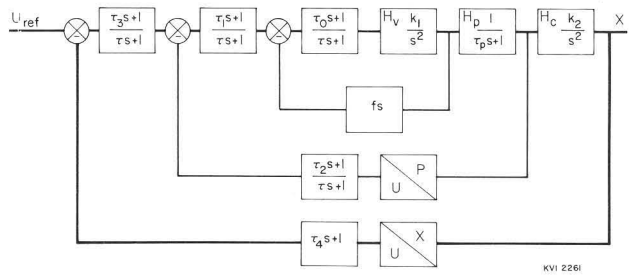

Fig. 3 : Block diagram of the control electronics showing the transfer function of the different parts. H_v is the simplified transfer function of the balanced valve. In fact due to the air flow there is a damping term. H_p reproduces the refill of the cylinder volume and H_c is Newton's law for the main piston with capacitor plate. The zeros of the correction networks serve to stabilise the three feedback loops.

pneumatic actuator and the control electronics form one system as shown in fig. 3. Here H_v and H_c are simplified transfer functions of the balanced valve and power cylinder, s is the Laplace operator. H_p is the transfer function connected with the pressure-build up in the cylinder. It is a fifth order control system.

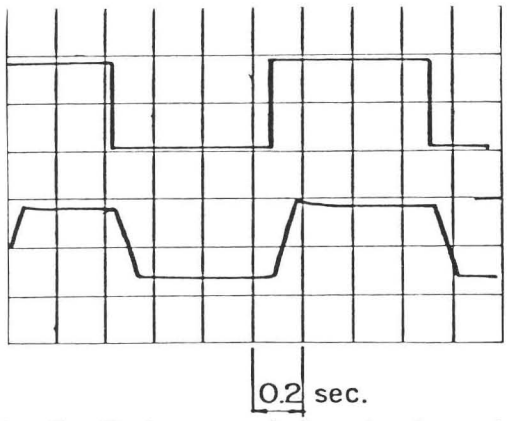

Fig. 4 : The displacement of the main piston, below, as function of a step positon signal. The small overshoot in the movement to one side is mainly due to a small drop in the stored air pressure and to the fact that the surface difference at both sides of the piston should be compensated in the circuitry following the pressure-voltage transducers.

The system is analysed using the root-locus technique. In first approximation the two inner feedback loops serve to lower the order of the system. From the correction networks the differentiating terms, zeros in the transfer function, are of main importance. The poles only serve to prevent a too strong overload of the amplifiers (not shown) and to smooth the ripple of the L.V.D.T. If the round trip amplification in the two inner loops is sufficiently large and if $\tau_3 = \tau_2$ then the whole system acts as a second order system. K_2 determines the natural frequency, $k_2 = w_n^2$, and τ_4 the damping. Both are adjusted to meet the speed and overshoot requirements. The time constants of the correction networks appear to be not critical. The displacement as function of a step position signal is shown in fig. 4. The possibility of small displacements of 0.1 mm has been checked. For small displacements, below 0.5 cm, the settling time to within 0.1 mm is below 0.1 s. The system is ideally suited too as a fast linear drive for scanning slits. In this case a cylinder with smaller diameter can be used which gives a higher speed.

New beam phase pick-up electrodes - A new probe head illustrated in fig. 5, has been built for the main cyclotron beam probe. It consists of a housing which contains a differential probe and two electrostatic pick-up plates located on both sides of the median plane, which are used for measuring the beam's RF phase.

RF amplifiers may be mounted in the probe head, close to the pick-up electrodes. However, experiments indicated that this did not improve the detection limit for beam signals when compared with the use of amplifiers located outside the vacuum chamber. The detection limit is determined by direct pick-up from the Dee rather than by noise or by signals introduced in the cabling.

The phase detector used in conjunction with this probe has been described in ref. 2. It uses synchronous detection of a deliberately introduced modulation of the beam in order to suppress beam unrelated RF

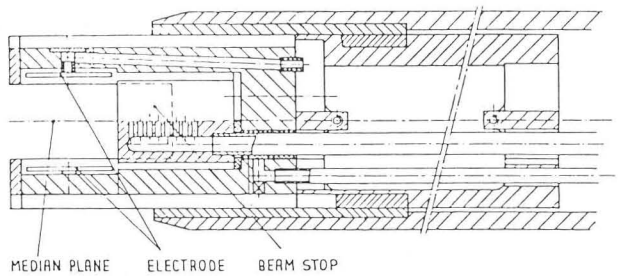

Fig. 5 : Longitudinal cross section of the beam probe head, showing pick-up electrodes and beam stop.

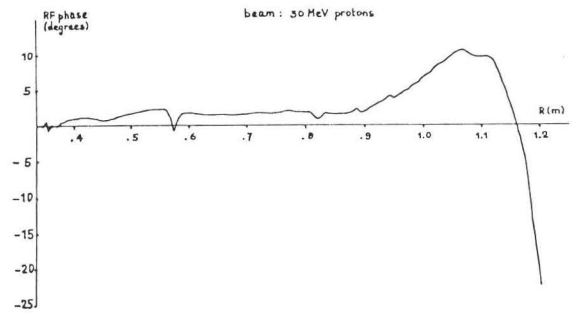

Fig. 6 : Beam RF phase as a function of radius.

signals. Modulation is achieved by periodically suppressing the beam with vertical deflecting plates in the cyclotron centre. The detector is capable of handling beam currents from 1 nA to 100 μA without range switching. Fig. 6 shows a trace of measured beam RF phase versus radius.

Studies on the KVI beam analysing system - The KVI beam analysing system consists of the following sequence of main components (see fig. 7): entrance slit S1, 105° double focusing analysing magnet AM, quadrupole doublet Q3A,Q3B, and exit slit S4. The doublet provides a horizontally enlarged image at the location of the exit slit of an intermediate image of the entrance slit, produced by the analysing magnet.

Experience accumulated in the past few years during experiments using the Q3D spectrograph indicated erratic behaviour of the energy resolution obtained from the analysing system. These experiences led to three specific questions:

i) Do we always have correct imaging by the quadrupole doublet.

ii) Is the imaging from entrance slit to exit slit sufficiently linear.

iii) To which degree is the resolution influenced by dispersion in the primary cyclotron beam.

While no final results are yet available on the third question, the first two have been successfully investigated. Here the main problem was how to measure the effect of possible aberrations without being hindered by dispersion, since a monoenergetic test beam was not available. This problem was solved in the following way. An extra slit (S2) was used to select a 2mrad divergence slice from the beam passed by the entrance slit. The location of this slice in the 10mrad divergence range could be chosen by moving the slit jaws. The magnetic spectrograph, without target, was set at zero degrees to determine the energy of each

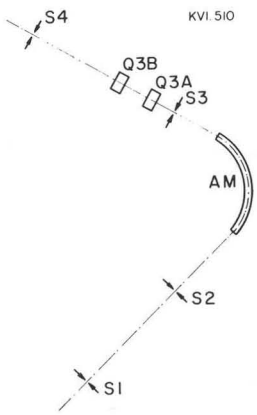

Fig. 7 : KVI beam analysing system
S1 = entrance slit, S2 = divergence slit
AM = 105° double focussing magnet
S3 = diaphragm at the position of image of S1
Q3A,Q3B = quadrupole doublet
S4 = exit slit

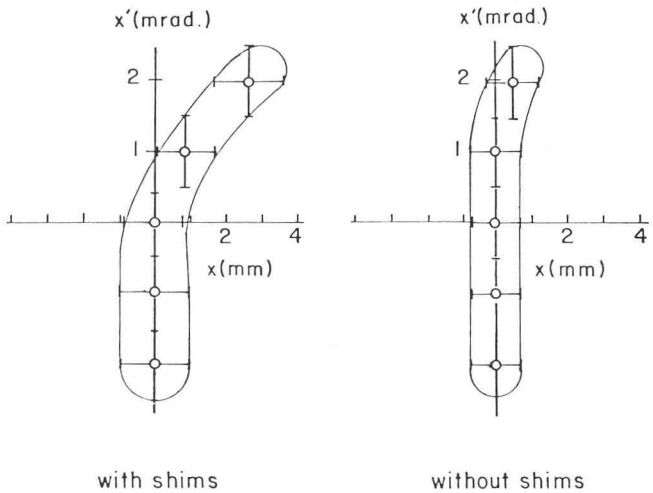

Fig.8 : Beam emittance of a 'mono-energetic' beam at the position of the exit slit, deduced from energy measurements of the transmitted beam.

slice in divergence space by looking at a fluorescent screen in its focal plane; here the position of the axial beam served as an energy reference. The observed energy difference was converted into the equivalent distance from the beam line axis at the exit slit, using the known dispersion of the analysing system. The meaning of this conversion is that for each divergence slice one determines the location of the image of the entrance slit for particles with the energy of the central ray. These locations, plotted in a single graph, constitute the beam emittance at the position of the exit slit that would be found for a monoenergetic cyclotron beam.

Measurements were performed on 50 MeV and 120 MeV alpha beams. In both cases data were taken for a number of excitations of the horizontally focusing quadrupole in the doublet (Q3A). In this way some redundancy was obtained and the lens setting for proper imaging could easily be found. No important discrepancies with the normally used settings were found.

A beam emittance at the exit slit, reconstructed in the way described above, is shown in fig. 8 (left). It is seen that the linearity of the image is far from perfect: particles with positive and negative divergence can not be focused on the exit slit at the same time. This distortion was suspected to arise from the entrance edge of the analysing magnet, which had been provided with a wedge shaped correction shim by the magnet manufacturer. First order estimates of the focusing effect of this shim based on measurements of the displacement of the effective field boundary indicated that the distortion would be reduced by removing the shim.

The result from measurements with the shim removed is shown in fig. 8 (right). It appears that the linearity of the imaging is not a determining factor anymore for the energy resolution that can be obtained. These results were subsequently confirmed during actual scattering experiments, when an overall energy resolution of 13 keV was obtained with 50 MeV alpha particles.

References.

1. R.H. Hidskes, J. Munneke, K.V.I. report "Trimplaatbesturing", June 1981 (in Dutch).
2. R.J. Vader, H.W. Schreuder, IEEE NS-26 (1979) 2205